Inclusive Baryon Production in e^+e^- Annihilation

M. Piccolo,[a] I. Peruzzi,[a] D. Lüke, V. Lüth, B. Richter, G. S. Abrams, M. S. Alam, A. Barbaro-Galtieri, A. M. Boyarski, M. Breidenbach, W. Chinowsky, J. M. Dorfan, R. Ely, G. J. Feldman, J. M. Feller, A. Fong, B. Gobbi, G. Goldhaber, G. Hanson, J. A. Jaros, A. D. Johnson, J. A. Kadyk,[b] B. P. Kwan, R. R. Larsen, P. LeComte, A. M. Litke, H. Lynch,[c] R. J. Madaras, J. F. Martin, D. H. Miller, H. K. Nguyen,[d] S. I. Parker, J. M. Paterson, M. L. Perl, T. P. Pun, P. A. Rapidis, M. T. Ronan, R. R. Ross, D. L. Scharre, R. F. Schwitters, W. Tanenbaum,[e] T. G. Trippe, G. H. Trilling, V. Vuillemin, J. E. Wiss, and D. E. Yount

Stanford Linear Accelerator Center and Department of Physics, Stanford University, Stanford, California 94305, and Lawrence Berkeley Laboratory and Department of Physics, University of California, Berkeley, California 94720, and Department of Physics and Astronomy, Northwestern University, Evanston, Illinois 60201, and Department of Physics and Astronomy, University of Hawaii, Honolulu, Hawaii 96822

(Received 21 October 1977)

The inclusive production of antiprotons and Λ's in e^+e^- annihilation has been measured as a function of the c.m. energy in the range 3.7–7.6 GeV. We find that the baryon cross section has a behavior different from the total hadronic production. Our results show a rapid rise in the ratio $\sigma_{\bar{p}}/\sigma_{\mu\mu}$ between 4.4 and 5 GeV, consistent with what would be expected from charmed baryon production. $\bar{\Lambda}$ production is 10–15% of $\bar{p}$ production at all energies.

We report here our measurements of the inclusive antiproton, Λ, and $\bar{\Lambda}$ production cross sections in e^+e^- annihilation. These measurements are important in their own right but are of particular interest now for they allow us to test the hypothesis that a new family of baryons—the charmed baryons—should be produced in e^+e^- collisions. These charmed baryons should undergo a chain of decays[1] and can have protons or Λ's among their decay products, thus giving an increase in the corresponding inclusive cross section when a threshold is passed.

The data sample used in this analysis consists of about 380 000 multihadronic events, corresponding to a total luminosity of about 37.3 pb^{-1}. These data were collected over a period of more than two and a half years using the Stanford Linear Accelerator Center–Lawrence Berkeley Laboratory magnetic detector at the e^+e^- storage ring SPEAR of the Stanford Linear Accelerator Center. The apparatus, trigger requirements, and event selection criteria have been described elsewhere.[2,3] A detailed description of the time-of-flight (TOF) system which provides the charged-particle identification for the analysis described below can be found in Peruzzi *et al.*[4]

To study antiproton production we have selected all multihadronic events with at least three detected charged prongs, and used TOF and momentum measurements to identify the particles. (Our analysis is restricted to antiprotons because protons have a large source of background from electroproduction on the residual gas in SPEAR.) The resolution of the TOF system is $\sigma = 0.35$ nsec, which corresponds to a K-p separation of 1σ at about 1.8 GeV/c; the proton identification is unambiguous (i.e., $>3\sigma$) up to 1.0 GeV/c. To make the maximum use of the TOF information and extend the particle identification to higher momenta on a statistical basis, we use a weighing technique.[5] From TOF and momentum measurement, we assign to each track a probability to be a pion, a kaon, or a proton, normalized so that the sum of the probabilities is unity. We then evaluate the total number of each kind of particle summing the respective probabilities for all tracks. For momenta up to 1 GeV/c, the number of antiprotons so obtained is the same as that obtained by a straight cut in the calculated mass of the tracks.

For momenta between 1 and 2 GeV/c we must correct for the resolution of the TOF system. We compute the 3×3 matrix of π, K, and p identification probabilities as a function of momentum (the diagonal elements give the probability that a particle is correctly identified while the off-diagonal elements give the misidentification probabilities). The inverse of this matrix relates the observed $\pi/K/p$ rates to the produced $\pi/K/p$ rates. From a Monte Carlo simulation we have found that this gives the correct number of antiprotons but with an error larger than the statistical one.

At momenta above 2 GeV/c the method deteri-

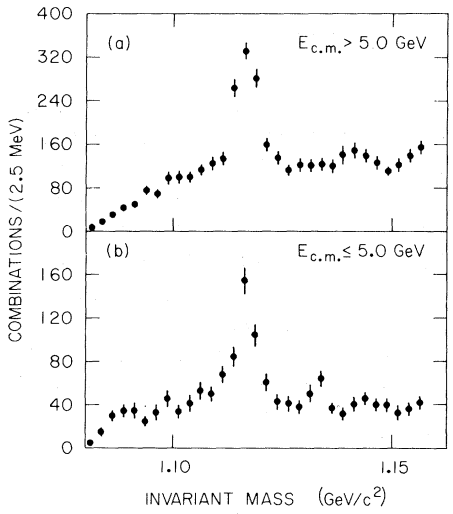

FIG. 1. $\bar{p}\pi^-$ and $\bar{p}\pi^+$ mass distribution for two c.m. energy ranges.

orates and the particle assignments are almost random. Hence, we use a Monte Carlo calculation to determine the fraction of antiprotons with momentum greater than 2 GeV/c. The fraction ranges from 0 at 4.2 GeV to 9% at 7.4 GeV. We assign an error to this correction equal to its value.

We next determine the efficiency for antiproton detection by a Monte Carlo calculation wherein pions, kaons, and nucleons are produced according to an isotropic phase-space model. The parameters of the model are adjusted at each energy to give the observed multiplicity and mean momentum of the data. The calculated detection efficiency for antiprotons ranges from 33% at 3.7 GeV to 50% at 7.4 GeV.

Λ and $\bar{\Lambda}$ are identified by studying the invariant-mass distribution of all two-prong, zero-charge combinations in an event (the electroproduction background from residual gas in the SPEAR vacuum chamber is not significant for Λ production). For a pair of tracks to be considered as a Λ or $\bar{\Lambda}$ candidate one of the prongs must have a TOF probability of $>1\%$ of being a p or $\bar{p}$ and the pair vertex must lie between 0.6 and 16 cm from the e^+e^- collision point (the Λ identification procedure is described more fully in Ref. 4). Figure 1 shows the two-particle mass distribution at low and high c.m. energies. The rms width of the peak is about 4 MeV as expected from our resolution. The Λ detection efficiency is also determined by a Monte Carlo calculation, and ranges from 12% at 3.7 GeV to 18% at 7.4 GeV (including the branching fraction to $p\pi$).

The proton and Λ detection efficiencies determined from the Monte Carlo calculation depend on the particle production model used in the calculation. We have used several models and estimate a systematic error of about ±25% in the efficiency calculation for both protons and Λ's. The main effect of this systematic error is on the overall normalization of the data; there is only a small effect between points nearby in energy.

Our results are summarized in Table I where,

TABLE I. $\bar{p}$ and Λ data summary. The third and sixth columns show numbers of observed events. The fourth column shows the number of observed antiprotons corrected for TOF misidentifications but not for detection efficiency. Systematic errors are not included.

$E_{c.m.}$ (GeV)	$\int \mathcal{L} dt$ (nb^{-1})	$N(\bar{p})$, $p < 1$ GeV/c	$N(\bar{p})$, weighted and corrected	$\sigma(\bar{p})$ (nb)	$N(\Lambda + \bar{\Lambda})$	$\sigma(\Lambda + \bar{\Lambda})$ (nb)
3.82	2650	424	707 ± 28	0.81 ± 0.03	61 ± 13	0.20 ± 0.04
4.03	2120	335	492 ± 25	0.66 ± 0.03	45 ± 10	0.18 ± 0.04
4.16	1670	266	442 ± 23	0.73 ± 0.04	28 ± 11	0.14 ± 0.06
4.28	850	112	222 ± 16	0.71 ± 0.05	24 ± 7	0.22 ± 0.06
4.41	2510	338	609 ± 28	0.64 ± 0.03	59 ± 13	0.19 ± 0.04
4.72	2210	376	733 ± 31	0.83 ± 0.04	57 ± 15	0.20 ± 0.05
5.32	1200	211	475 ± 27	0.92 ± 0.05	33 ± 10	0.20 ± 0.06
5.86	1970	275	619 ± 46	0.67 ± 0.05	58 ± 10	0.18 ± 0.03
6.23	3440	417	1114 ± 89	0.66 ± 0.05	78 ± 15	0.14 ± 0.03
6.59	4100	431	1224 ± 102	0.58 ± 0.05	114 ± 18	0.16 ± 0.02
7.04	5520	646	1715 ± 155	0.57 ± 0.05	120 ± 19	0.12 ± 0.02
7.36	8790	835	2425 ± 239	0.49 ± 0.05	250 ± 26	0.16 ± 0.02

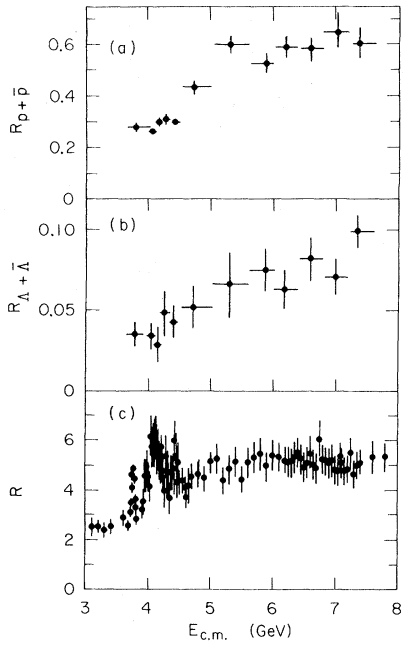

FIG. 2. (a) $R(p+\bar{p}) = 2\sigma(\bar{p})/\sigma_{\mu\mu}$ vs c.m. energy. (b) $R(\Lambda+\bar{\Lambda}) = \sigma(\Lambda+\bar{\Lambda})/\sigma_{\mu\mu}$ vs c.m. energy. (c) $R_H = \sigma_{had}/\sigma_{\mu\mu}$ vs c.m. energy from previous work. Radiative corrections have been made and the large peaks due to the ψ and ψ' have been omitted.

for each c.m. energy interval, we give the number of antiprotons with momentum lower than 1.0 GeV/c, the total number of antiprotons determined by the weight method, corrected for those with $p > 2$ GeV/c, the number of detected Λ's, the luminosity, and the cross sections (errors do not include efficiency uncertainties).

In Fig. 2(a) we plot $R(p+\bar{p}) = 2\sigma_{\bar{p}}/\sigma_{\mu\mu}$, the ratio of the inclusive charged-nucleon cross section to the μ-pair production cross section, versus c.m. energy. Figure 2(b) shows $R(\Lambda+\bar{\Lambda}) = \sigma(\Lambda+\bar{\Lambda})/\sigma_{\mu\mu}$ while Fig. 2(c) shows for comparison $R_H = \sigma_{tot}$ (hadron)$/\sigma_{\mu\mu}$ as determined previously in the same detector.[6]

$R(p+\bar{p})$ increases by about a factor of 2 from roughly 0.3 to 0.6 between 4.4 and 5 GeV in c.m. energy. $R(\Lambda+\bar{\Lambda})$ appears to have a similar behavior though statistical errors are much worse and preclude any precise comparison. $R(\Lambda+\bar{\Lambda})$ is about 10–15% of $R(p+\bar{p})$ at all energies. R_H, on the other hand, increases by a factor of about 2 around 4 GeV and has a complex structure which has been identified as corresponding to the onset of production of charmed mesons and charmed meson resonances.[5]

The fact that the increase in $R(p+\bar{p})$ occurs above 4.4 GeV while the increase in R_H occurs around 4 GeV gives us confidence that the baryon effect is not due to some subtle particle misidentification problem in the TOF system, and, therefore, that some new baryon production mechanism is coming into play above 4.4 GeV. Such a mechanism could be the production of singly charmed, strangeness-0 or -1 baryons whose thresholds are expected to lie in this range. Indeed, a particle with the expected properties of such a charmed baryon has been observed in photoproduction[7] and neutrino experiments.[8]

The most direct evidence for the production of charmed baryons in e^+e^- annihilation would be the observation of a peak in the mass distribution of those particles which would be expected in the decays of such baryons. We have not observed such a peak. However, the acceptance of the magnetic detector for the expected decay modes is low and our inability to find a peak is not inconsistent with charmed baryon production.

If the increase in the inclusive cross sections is due to charmed baryon production, our measurements indicate that the ratio of charmed baryon to charmed meson production is about the same as the ratio of uncharmed baryon to uncharmed meson production. Further, with the same assumption, the small value of $\Delta R(\Lambda+\bar{\Lambda})/\Delta R(p+\bar{p})$ indicates that the weak decays of charmed baryons must go preferentially to particle combinations containing p, n, or $\Sigma^{\pm}$ and not to Λ or Σ^0. Since it is very difficult to conceive of a mechanism which would make charmed baryons preferentially to $\Sigma^{\pm}$ and not to Σ^0, it is likely that the preferred decay mode is nucleon plus strange meson and pions.

We acknowledge the support of the Deutsche Forschungsgemeinschaft, the Laboratori Nazionali de Frascati dell'Istituto Nazionale di Fisica Nucleare, and the Swiss National Science Foundation. The work was also supported in part by the U. S. Department of Energy.

---

[a]Present address: Laboratori Nazionali di Frascati dell'Istituto Nazionale di Fisica Nucleare, Rome, Italy.

[b]Present address: CERN, Geneva, Switzerland.

[c]Present address: DESY, Notkestieg 1, Hamburg, Germany.

[d]Present address: Laboratoire de Physique Nucléaire et Hautes Energies, Université Paris VI, Paris, France.

[e]Present address: Physics Department, Harvard

University, Cambridge, Mass.

[1]See, for example, A. De Rújula *et al.*, Phys. Rev. D 12, 147 (1975); B. W. Lee *et al.*, Phys. Rev. D 15, 157 (1977).

[2]J.-E. Augustin *et al.*, Phys. Rev. Lett. 34, 233 (1975); F. Vannucci *et al.*, Phys. Rev. D 15, 1814 (1977).

[3]A. Barbaro-Galtieri *et al.*, Phys. Rev. Lett. 39, 1058 (1977).

[4]I. Peruzzi *et al.*, to be published.

[5]G. Goldhaber *et al.*, Phys. Rev. Lett. 34, 419 (1975); I. Peruzzi *et al.*, Phys. Rev. Lett. 37, 569 (1976); G. J. Feldman *et al.*, Phys. Rev. Lett. 38, 1313 (1977); G. Goldhaber *et al.*, Phys. Lett. 69B, 503 (1977).

[6]J. Siegrist *et al.*, Phys. Rev. Lett. 36, 526 (1976); R. F. Schwitters, in *Proceedings of the International Symposium on Lepton and Photon Interactions at High Energies, Stanford, California, 1975*, edited by W. T. Kirk (Stanford Linear Accelerator Center, Stanford, Calif., 1975); P. A. Rapidis *et al.*, Phys. Rev. Lett. 39, 526, 974(E) (1977).

[7]B. Knapp *et al.*, Phys. Rev. Lett. 37, 882 (1976).

[8]E. G. Cazzoli *et al.*, Phys. Rev. Lett. 34, 1125 (1975).

Possibility of Charmed Hypernuclei

C. B. Dover and S. H. Kahana
Brookhaven National Laboratory, Upton, New York 11973
(Received 10 August 1977)

We suggest that both two-body and many-body bound states of a charmed baryon and nucleons should exist. Estimates indicate binding in the $^1S_0$ state of C_1N ($I=\frac{3}{2}$) and SN ($I=1$). We further estimate the binding energy of C_0, C_1 in various finite nuclei.

Recent experiments[1] have established the existence of a new class of mesons and baryons possessing net charm. In particular, there is firm evidence for the charmed baryons $B_c = C_0$, C_1 (Λ_c and Σ_c) and the charmed mesons, D, D^*. It is hence of fundamental interest to establish the nature of the interactions of these charmed particles with more familiar hadrons.

In this Letter we ask whether the charmed baryons will bind to a single nucleon or to finite nuclei, producing charmed analogs of the deuteron or of hypernuclei. The estimated short lifetime of even the lowest-mass charmed baryon, $\tau(C_0) \sim 10^{-11}-10^{-14}$ sec, may make it difficult to establish the existence of such analog bound states. These questions are discussed here in a nonrelativistic framework in which the B_c-nucleon interaction is represented by a sum of single-boson-exchange potentials. The B_c-nucleus potential is obtained by averaging the B_c-N interaction over the nuclear density. The large mass of the charmed baryon alters the dynamics appreciably, resulting in a reduction in the B_c kinetic energy for both two- and many-body systems. Thus, in the B_c-nucleus case, where we find potentials comparable to the nucleon-nucleus potential in depth, a rich spectroscopy emerges encompassing many bound levels.

The B_c-N potential, $V(r)$, is given by a sum of meson exchange potentials for $r \geq r_c$ but taken phenomenologically as an infinite hard core for $r \leq r_c$. Such models have frequently been applied to nucleon-nucleon (NN) scattering in the low-energy region.[2] Recently, a one-boson-exchange model has been constructed[3] which successfully reproduces both low-energy NN and hyperon-nucleon (ΛN and ΣN) data. This model includes the coupling of SU(3) nonets of pseudoscalar, scalar, and vector mesons to the $\frac{1}{2}^+$ baryon octet of SU(3). We use here a natural generalization of this model which considers the coupling of mesons obtained by mixing the $\{15\}$ and $\{1\}$ representations of SU(4) with members of the $\{20\}$ representation of $\frac{1}{2}^+$ baryons. The details are given by Dover, Kahana, and Trueman.[4]

We have restricted out attention to the four lightest singly charmed baryons C_0, C_1, A, and S with isospin $T=0$, 1, $\frac{1}{2}$, and $\frac{1}{2}$, respectively. For the C_0 (also called Λ_c), we take the presumed experimental mass of $M_{C_0} = 2.26$ GeV; for C_1 (also called Σ_c), we take $M_{C_1} = 2.42$ GeV. For A and S, we use theoretical estimates[5] of $M_A = 2.47$ GeV and $M_S = 2.57$ GeV. Since only the C_0 baryon is stable under strong interactions it is likely that the C_0-N and C_0-nucleus systems are of greatest interest, although the C_1 nuclei are most strongly bound.

Using these potentials we have searched for B_cN bound states by solving the nonrelativistic Schrödinger equation. The meson-nucleon and meson-B_c coupling constants we use are listed in Table II of Ref. 4 and Table I of Ref. 3. We took $r_c = 0.522$ fm for $^1S_0$ states.

We start by considering the $^1S_0$ state of B_cN